DOI: http://dx.doi.org/10.22104/ijhfc.2016.394

Iranian Journal of Hydrogen & Fuel Cell 2(2016) 113-125

Iranian Journal of Hydrogen & Fuel Cell

IJHFC

Journal homepage://ijhfc.irost.ir

How to design a cryogenic Joule-Thomson cooling system: case study of small hydrogen liquefier

Ali Saberimoghaddam*, Mohammad Mahdi Bahri Rasht Abadi

Department of Chemistry and Chemical Engineering, Faculty of Chemical Engineering, Malek Ashtar University of Technology (MUT), Lavizan, Tehran, Iran

Article Information

Article History:

Received:
5 Oct 2016
Received in revised form:
9 Nov 2016
Accepted:
19 Nov 2016

Keywords

Refrigeration
Joule-Thomson
Hydrogen liquefaction
Heat exchanger
Design and simulation

Abstract

Heat exchangers are the critical components of refrigeration and liquefaction processes. Selection of appropriate operational conditions for the cryogenic recuperative heat exchanger and expansion valve operating in a Joule-Thomson cooling system results in improving the performance and efficiency. In the current study, a straightforward procedure is introduced to design an efficient Joule-Thomson cooling system. Determining the appropriate operational conditions and configuration of streams within the recuperative heat exchanger are discussed comprehensively. A Joule-Thomson cooling system including a helically coiled tube in the tube heat exchanger and expansion valve was considered as a case study. Simulation was performed by a procedure different from the conventional finite element method and the results were validated versus data obtained from a small laboratory hydrogen liquefier. In accordance with mathematical modeling performed on the recuperative heat exchanger, it is better to flow low pressure hydrogen inside the inner tube and high pressure hydrogen within the annulus. This arrangement results in needing shorter length heat exchanger tubes as compared with the reverse arrangement.

1. Introduction

Small Joule-Thomson cryogenic coolers (Cryo-Coolers) have been studied during the three past decades [1]. These systems are generally used in radiation detectors, medical research, aerospace sciences, etc. [2]. Moreover, Joule-Thomson cooling systems (JTC systems) are used in small gas liquefaction units such as helium and hydrogen liquefiers [3]. These systems typically include recuperative a heat exchanger and Joule-Thomson expansion valve [4]. The JTC systems are used as the main source of refrigeration in cryogenic gas liquefiers. The efficiency of these systems depends strongly on the recuperative heat exchanger used [5].

*Corresponding Author's Fax:+982122962257
E-mail address: articlemut@gmail.com

These systems traditionally use a certain mechanism to create cooling, as shown in Fig. 1. As can be seen, the warm high-pressure gas enters the recuperative heat exchanger and exchanges heat with the cold gas returning from the other side of the recuperative heat exchanger. Then, the high pressure gas passes through an expansion valve and due to the Joule-Thomson effect, the gas partially transforms into liquid.

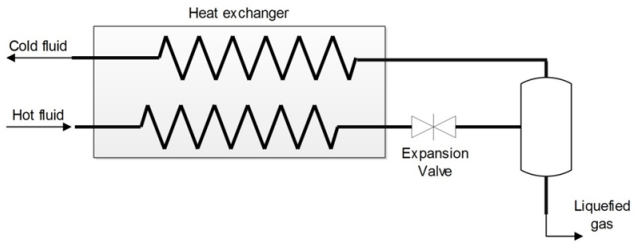

Fig. 1. The Joule-Thomson cooling system including a recuperative heat exchanger, expansion valve and collector.

Extensive studies have been carried out on JTC systems, and almost all the studies have been focused on the recuperative heat exchanger [6-10]. Pacio and Dorao [11] reviewed the thermal hydraulic models of cryogenic heat exchangers. They introduced physical effects, such as changes in fluid properties, flow maldistribution, axial longitudinal heat conduction, and heat leakage, as the main challenges of cryogenic heat exchangers. Aminuddin and Zubair [12] studied the various losses in a cryogenic counter current heat exchanger numerically. They discussed the effect of longitudinal heat conduction loss as a parasitic heat loss by conduction from heat exchanger cold end to the adjacent components, but they did not perform any experimental tests. Krishna et al. [13] studied the effect of longitudinal heat conduction in the separating walls on the performance of a three-fluid cryogenic heat exchanger with three thermal communications. They illustrated that the thermal performance of heat exchangers operating at cryogenic temperature is strongly governed by various losses such as longitudinal heat conduction through the wall, heat in-leak from the surroundings, flow maldistribution, etc.

Gupta et al. [14] investigated the second law analysis for counter current cryogenic heat exchangers in the presence of ambient heat in-leak and longitudinal heat conduction through the wall. They cited the importance of considering the effect of longitudinal heat conduction in the design of cryogenic heat exchangers. Nellis [15] presented a numerical model of a heat exchanger in which the effect of axial conduction, property variations, and parasitic heat losses to the environment have been explicitly modeled. He concluded that small degradation exists in the performance of a heat exchanger in conditions where the temperature of the heat exchanger cold end is equal to the temperature of the inlet cold fluid. Narayanan and Venkatarathnam [16] presented a relationship between the effectiveness of a heat exchanger losing heat at the cold end. They studied a Joule-Thomson cryo-cooler and concluded that the hot fluid outlet temperature will be lower in heat exchangers with heat in-leak at the cold end with respect to heat exchangers with insulated ends. Ranganayakulu et al. [17] studied the effect of longitudinal heat conduction in a compact plate fin and tube fin heat exchanger using the finite element method. They indicated that the thermal performance deteriorations of the cross flow plate-fin, cross flow tube-fin and counter flow plate-fin heat exchangers due to longitudinal heat conduction may become significant, especially when the fluid capacity rate ratio is equal to one and when the longitudinal heat conduction parameter is large.

Damle and Atrey [18] studied the effect of reservoir pressure and volume on the cool-down behavior of a miniature Joule–Thomson cryo-cooler considering the distributed Joule-Thomson effect. According to their research, these parameters affect the cool down time, cooling effect and the time for which the cooling effect is obtained at the required cryogenic temperature. Chou et al. [19] used a simplified transient one-dimensional model of momentum and energy transport to simulate the flow and heat transfer characteristics. They proposed that

the size and weight, as important parameters, of the cryo-cooler must be reduced to improve the performance. Tzabar and Kaplansky [20] presented a numerical cool-down analysis for Dewar-detector assemblies cooled with Joule-Thomson cryo-coolers. They analyzed the ability of their numerical model in predicting the cool-down performances of Joule-Thomson cryo-coolers during the development stages prior to prototype production. Hong et al. [21] studied the cool-down characteristics of a miniature Joule-Thomson refrigerator with a pressurized vessel, which has different initial pressures of nitrogen gas. They discussed on the influence of supply pressure and temperature on the mass flow rate during the cool-down stage.

In this paper, the JTC systems operating in the small hydrogen Liquefiers has been discussed. The helically coiled tube in a tube heat exchanger was used to study the problem. This type of heat exchanger is appropriate for small-scale gas liquefiers. Study of the effective parameters to design and enhance the efficiency of JTC systems and conducting appropriate design procedure are the main subjects of this research. In addition, a straightforward procedure has been conducted to determine the appropriate operational conditions for a Joule-Thomson cooling system operating in a small hydrogen liquefier.

2. Design procedure

In order to study the JTC systems, two important notes must be considered. The first one is selection of a suitable equation of state, and the second one is the design of a recuperative heat exchanger, considering variable properties of gas along the heat exchanger tubes. The Modified Benedict-Webb-Rubin (MBWR) equation of state was selected due to its appropriate estimation of hydrogen properties at cryogenic temperatures [22]. The MBWR equation of state was developed in 1987 by Younglove for hydrogen gas as an equation of state with 32 parameters as follows [23]:

(1)

$$
\begin{aligned}
&= CRT + \rho^2\left(G(1)T + G(2)T^{\frac{1}{2}} + G(3) + \frac{G(4)}{T} + \frac{G(5)}{T^2}\right)\\
&+\rho^3\left(G(6)T + G(7) + \frac{G(8)}{T} + \frac{G(9)}{T^2}\right)\\
&+\rho^4\left(G(T)T + G(11) + \frac{G(12)}{T}\right) + \rho^5\left(G(13)\right)\\
&+\rho^6\left(\frac{G(14)}{T} + \frac{G(15)}{T^2}\right) + \rho^7\left(\frac{G(16)}{T}\right) + \rho^8\left(\frac{G(17)}{T} + G(18)T^2\right)\\
&+\rho^9\left(\frac{G(19)}{T^2}\right) + \rho^3\left(\frac{G(20)}{T^2} + \frac{G(21)}{T^3}\right)\exp\left(\gamma\rho^2\right)\\
&+\rho^5\left(\frac{G(22)}{T^2} + \frac{G(23)}{T^4}\right)\exp\left(\gamma\rho^2\right)\\
&+\rho^7\left(\frac{G(24)}{T^2} + \frac{G(25)}{T^3}\right)\exp\left(\gamma\rho^2\right) + \rho^9\left(\frac{G(26)}{T^2} + \frac{G(27)}{T^4}\right)\\
&\exp\left(\gamma\rho^2\right) + \rho^{11}\left(\frac{G(28)}{T^2} + \frac{G(29)}{T^3}\right)\exp\left(\gamma\rho^2\right)\\
&+\rho^{13}\left(\frac{G(30)}{T^2} + \frac{G(31)}{T^3} + \frac{G(32)}{T^4}\right)\exp\left(\gamma\rho^2\right)
\end{aligned}
$$

Where, ρ is the density of hydrogen, R is the universal constant of gases, T is the temperature, and γ is the heat capacity ratio. The values of G for hydrogen gas have been presented in Table 1.

Table 1. The values of G parameters for hydrogen gas, used in the MBWR equation of state [24]

Para.	Value	Para.	Value	Para.	Value	Para.	Value
G(1)	4.675528393416E-05	G(9)	5.161197159532E+00	G(17)	4.051941401315E-10	G(25)	1.206839307669E-04
G(2)	4.289274251454E-03	G(10)	1.999981550224E-08	G(18)	1.157595123961E-07	G(26)	-3.841588197470E-08
G(3)	-5.164085596504E-01	G(11)	2.896367059356E-05	G(19)	-1.269162728389E-09	G(27)	-4.036157453608E-06
G(4)	2.961790278010E-01	G(12)	-2.257803939041E-01	G(20)	-4.983023605519E+00	G(28)	-1.250868123513E-11
G(5)	-3.027194968412E+00	G(13)	-2.287392761826E-07	G(21)	-1.606676092098E+01	G(29)	1.976107321880E-10
G(6)	1.908100320379E-06	G(14)	2.446261478645E-06	G(22)	-1.926799185310E-02	G(30)	-2.411883474011E-14
G(7)	-1.339776859288E-04	G(15)	-1.718181601119E-04	G(23)	9.319894638928E-01	G(31)	-4.127551498251E-14
G(8)	3.056473115421E-02	G(16)	-5.465142603459E-08	G(24)	-3.222596554434E-05	G(32)	8.917972883610E-13

In common hydrogen liquefiers, two steps of catalytic ortho-para conversion are commonly carried out using an iron oxide catalyst. The first step is performed in a liquid nitrogen bath (pre-cooling section). The value of the para-hydrogen content in this step can reach up to 50%. For this reason, in the simulations performed here, the high-pressure hydrogen which enters the Joule-Thomson cooling system was assumed at 50% para-hydrogen. The second step can be carried out by two procedures; the catalyst can be coated on the heat exchanger surface area to perform catalytic conversion in the gaseous state (common in big scale hydrogen liquefiers) or the catalyst can be placed in the collector to convert liquefied hydrogen into liquid para-hydrogen (common in small scale hydrogen liquefiers). In our small hydrogen liquefier, the second step of conversion has not been performed. Therefore, validation against experimental data was carried out considering hydrogen as 50 % para-hydrogen (high-pressure and low-pressure gas). The properties of hydrogen such as density, heat capacity, viscosity, and thermal conductivity were collected from references [24]. The collected data in the form of fitted correlations were used to evaluate hydrogen properties versus temperature along the heat exchanger tubes. The data presented by McCarty are commonly used for engineering design calculations. Therefore, the fitted correlations can be used to evaluate the properties of hydrogen along the heat exchanger tubes. The correlation coefficients (R^2) are greater than 0.98 for all achieved equations. These equations are presented in Table 2.

MATLAB programming was used to simulate the recuperative heat exchanger. As mentioned above, the equations presented in Table 2 were used to evaluate the various properties of hydrogen in the differential segments as shown in Fig. 2.

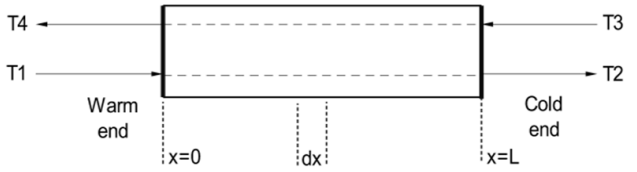

Fig. 2. The differential segment of the recuperative heat exchanger.

A helically coiled tube in the tube heat exchanger was selected due to its appropriate features for small scale liquefiers. The details of the heat exchanger are shown in Fig. 3.

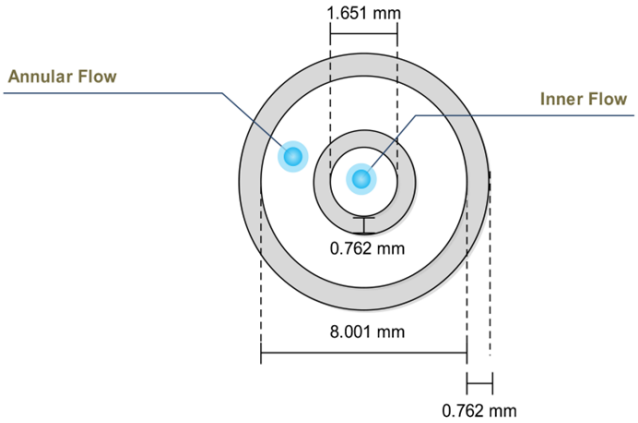

Fig. 3. The cross section of the tubes used in the recuperative heat exchanger.

Table 2. The fitted correlations for determining the various properties of hydrogen gas

Parameters	The fitted correlations
Specific heat of hydrogen at 80 bar	$Cp_{HP}=1.64103\times10^{-5}\times T^4-3.3074706\times10^{-3}\times T^3+0.2343332389\times T^2-6.7234569913\times T+78.2528012405$
Viscosity of hydrogen at 80 bar	$\mu_{HP}=5.324375\times10^{-9}\times T^2 - 6.88339636\times10^{-7}\times T + 2.6974296271\times10^{-5}$
Density of hydrogen at 80 bar	$\rho_{HP}=8.6084724\times10^{-3}\times T^2 - 1.9676470642\times T + 124.2009885257$
Thermal conductivity of hydrogen at 80 bar	$k_{HP}=4.61872221\times10^{-7}\times T^3-5.2709958383\times10^{-5}\times T^2+5.64228018517\times10^{-4}\times T+0.146426434369161$
Specific heat of hydrogen at 1.2 bar	$Cp_{LP}=-5.1877817\times10^{-8}\times T^5+1.4364245164\times10^{-5}\times T^4-1.554228186978\times10^{-3}\times T^3+8.2686154056125\times10^{-2}\times T^2-2.176241287404820\times T+33.358740091784000$
Viscosity of hydrogen at 1.2 bar	$\mu_{LP}=-2\times10^{-10}\times T^2 + 5.94\times10^{-8}\times T - 5.11\times10^{-8}$
Density of hydrogen at 1.2 bar	$\rho_{LP}=-9.863995035\times10^{-6}\times T^3+1.885706731205\times10^{-3}\times T^2 -0.125766289439548\times T+3.378978750152610$
Thermal conductivity of hydrogen at 1.2 bar	$k_{LP}=-1.015999341\times10^{-6}\times T^2 + 7.75359205961\times10^{-4}\times T + 2.335591159376\times10^{-3}$

Hydrogen mass flow rate within the inner tube was chosen as 0.25 kg h^{-1}. This mass flow rate has been used to produce 500 cc h^{-1} liquid hydrogen in our small hydrogen liquefier at the MUT cryogenic laboratory. The heat transfer surface area was calculated with the assumption of 50 J m^{-2} heat leakage from the ambient to recuperative heat exchanger (ultra-high vacuum condition without radiation shields). The LMTD method with the new approach was used to determine the needed heat transfer surface area in each differential segment. In this procedure, the temperature range of one side of the heat exchanger was divided into several individual segments and the corresponding temperatures of the heat exchanger's other side were calculated based on the energy balance. This procedure was used for all individual differential segments, and eventually temperatures at different points of the heat exchanger tube were evaluated. Using this method, it is possible to calculate the appropriate length for a heat exchanger with an unknown cold fluid outlet temperature (in the conventional finite element method the length of the heat exchanger must be specified for the model). In order to estimate the convection heat transfer coefficient within the helical coiled tube, the correlations proposed by Xin and Ebadian were used as follows [25]:

$$Nu_{ave} = 0.00619 Re^{0.92} Pr^{0.4} \left(1 + \frac{3.455d}{D_{coil}}\right) \quad (2)$$

$$5\times10^{3} < Re < 10^{5},\ 0.7 < Pr < 5,\ 0.0267 < \frac{d}{D_{coil}} < 0.0884$$

$$Nu_{ave} = \left(2.153 + 0.318 De^{0.643}\right) Pr^{0.177} \quad (3)$$

$$20 < De < 2000,\ 0.7 < Pr < 175,\ 0.0267 < \frac{d}{D_{coil}} < 0.0884$$

The parameters used for modeling and simulating the recuperative heat exchanger have been presented in Table 3.

In this study, the JTC system, including recuperative heat exchanger and expansion valve, is a part of the hydrogen liquefaction unit shown in Fig. 4 (highlighted by a bold line in PFD). As can be seen, the compressed hydrogen cools within the initial heat exchanger and liquid nitrogen (LN_2) bath, respectively. Then, hydrogen gas enters the JTC system.

Table 3. Parameters used for modeling the recuperative heat exchanger

Parameter	Value
Mass flow of high pressure hydrogen (kg/h)	0.25
Mass flow of low pressure hydrogen (kg/h)	0.21
Liquefaction efficiency (%)	~ 16
Temperature interval of high pressure side (K)	1
Flow pressure of the high pressure side (bar)	80
Flow pressure of the low pressure side (bar)	1.2
Heat leak to heat exchanger(W)	0

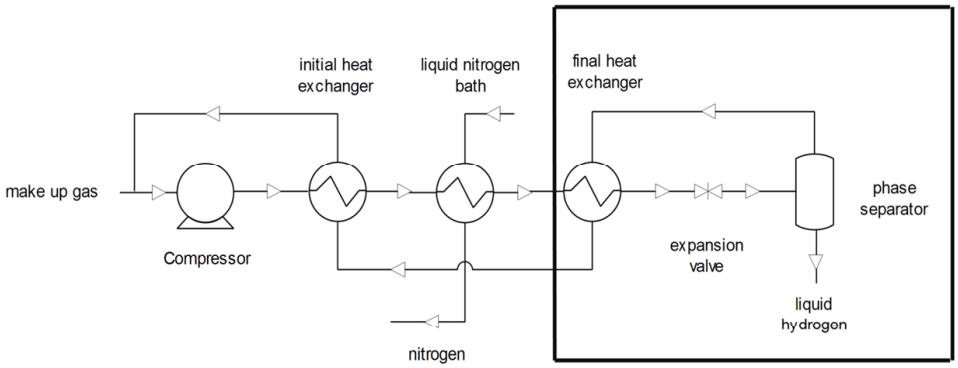

Fig. 4. The PFD of the small scale hydrogen liquefaction unit.

In order to validate the model, a simulated Joule-Thomson cooling system was manufactured and tested in an actual gas liquefier. The manufactured system is shown in Fig. 5. Stainless steel 304L was used in the recuperative heat exchanger material and the system was placed in an evacuated cold-box.

Fig. 5. Joule-Thomson cooling system manufactured according to simulation results.

The details of the experiment are presented in Table 4. The expansion valve inlet temperatures obtained from the gas liquefier were lower than those obtained from the simulation. This phenomenon can be attributed to the constant value of heat leakage (50 J m^{-2}) applied in the simulation. This value is lower at points with higher temperatures along the heat exchanger.

Table 4. The details of the manufactured Joule-Thomson cooling system

Parameters	Values
Working fluid	Hydrogen
Mass flow rate (kg h^{-1})	0.25
Inner tube internal diameter (mm)	1.671
Outer tube internal diameter (mm)	8.001
Tubes wall (mm)	0.762
Tube length (m)	2.8
Tube wall thermal conductivity (W m^{-1} K^{-1})	50

Moreover, longitudinal heat conduction along the tube wall was neglected in the simulation. In the case of a long heat exchanger, longitudinal heat conduction along the tube wall decreases the tube outlet temperature.

3. Result and discussion

3.1. Determining the Operational Conditions

Due to the negative Joule-Thomson coefficient of hydrogen at ambient temperatures, all hydrogen liquefiers use a pre-cooling system. The precooling is usually performed using liquid nitrogen (LN_2) because of its low-cost and safety aspects. The normal boiling point of nitrogen is around 78 K and can be decreased to around 65 K by decreasing the bath pressure to 0.2 bar (vacuum conditions). Therefore, if the hydrogen gas passes through the vacuum LN_2 bath before entering the JTC section of liquefier, its temperature can be decreased to around 65 K (with an effectiveness of 100 %) or 69 K (with an effectiveness of 90 %). In this study, an effectiveness of 90 % was considered for the LN_2 bath in accordance with tests performed by our small hydrogen liquefier. The temperature of high pressure hydrogen gas after passing through the LN_2 bath is around 69 K based on the regarded effectiveness. The temperature and pressure of various streams in the JTC section of the hydrogen liquefier are shown in Fig. 6. Unknown values must be determined to design an efficient hydrogen liquefier. Since the expansion valve outlet is partially liquid hydrogen, its temperature is equal to liquid hydrogen. In order to transfer liquid hydrogen into a storage tank without a cryogenic pump, the pressure of the expansion valve outlet should be adjusted higher than atmospheric pressure. Here, the pressure of expansion valve outlet was adjusted to 1.2 bar. The corresponding saturated temperature is around 21 K at the expansion valve outlet. According to data obtained from our small hydrogen liquefier, the pressure drop within the heat exchanger tubes is negligible.

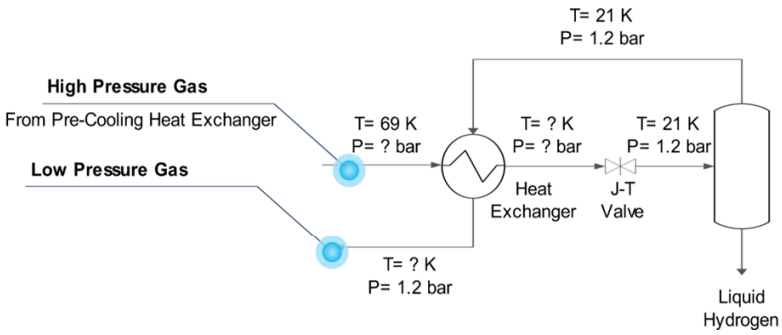

Fig. 6. The specified and unspecified temperature and pressure of various streams in the Joule-Thomson cooling system.

If all the streams are assumed independent, the unknown temperatures may be easily evaluated by establishing energy balance as follows:

$$m_i C_i \left(T_{i-in} - T_{i-out}\right) = m_o C_o \left(T_{o-out} - T_{o-in}\right) \quad (4)$$

Where mi is the mass flow rate of the high pressure hydrogen (warm gas), C_i is the mean specific heat of the warm gas, mo is the mean mass flow rate of the cold gas, C_o is the mean specific heat of the cold gas, T_{i-in} is the temperature of the inlet warm stream, T_{i-out} is the temperature of the outlet warm stream, T_{o-in} is the temperature of the inlet cold stream, and T_{o-out} is the temperature of the outlet cold stream. Due to dependency of various streams in the JTC system, equation (4) can be changed to equation (5) as follows:

(5)

$$m_i C_i \left(T_{i-in} - T_{i-out}\right) = m_i (1 - x[T_{i-out}, P_{i-out}]) C_o \left(T_{o-out} - T_{o-in}\right)$$

Where $x[T_{i-out},P_{i-out}]$ is the liquid fraction of hydrogen in the expansion valve outlet as a function of T_{i-out} and P_{i-out}. P_{i-out} is the pressure of hydrogen gas in the expansion valve inlet. The temperature and pressure of expansion valve inlet influences the liquid fraction of outlet. This phenomenon takes place due to the variable Joule-Thomson coefficient as follows:

$$\mu_{J-T} = \left(\frac{\partial T}{\partial P}\right)_h \quad (6)$$

Fig. 7 shows the isenthalpic curves for a real gas at different temperatures and pressures. The slope of the tangent line on the isenthalpic curves presents the value of the Joule-Thomson coefficient at any temperature and pressure.

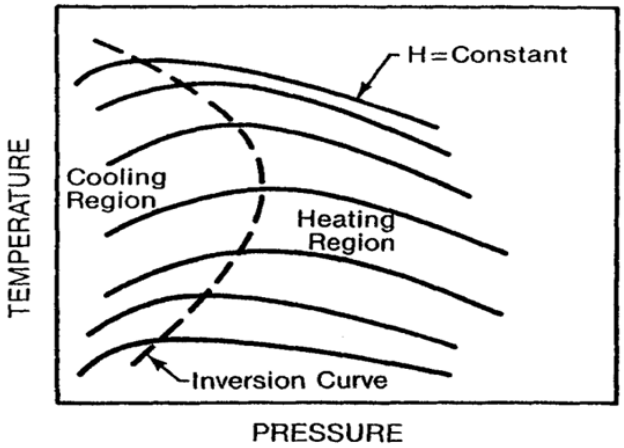

Fig. 7. Isenthalpic curves of a real gas and inversion temperature.

Fig. 8 shows the liquid fraction of hydrogen at the expansion outlet versus the operational pressure for various temperature of gas entering the expansion valve. As can be seen, at any temperature that hydrogen enters the expansion valve, there is a pressure where the liquid fraction of hydrogen is maximum. The locus of the liquid fraction maximums is also shown in Fig. 8. At any pressure, the lower temperature of gas entering the expansion valve results in a higher liquid fraction value. This means that the recuperative heat exchanger should have sufficiently high effectiveness to keep the outlet warm stream temperature as low as possible. The lower temperatures result in higher liquid fractions in the expansion valve outlet. Consequently, the higher effectiveness of the recuperative heat exchanger leads to a higher overall efficiency of the whole unit. Figure 8 shows that the maximum hydrogen liquefaction occurs when the temperature and pressure of the

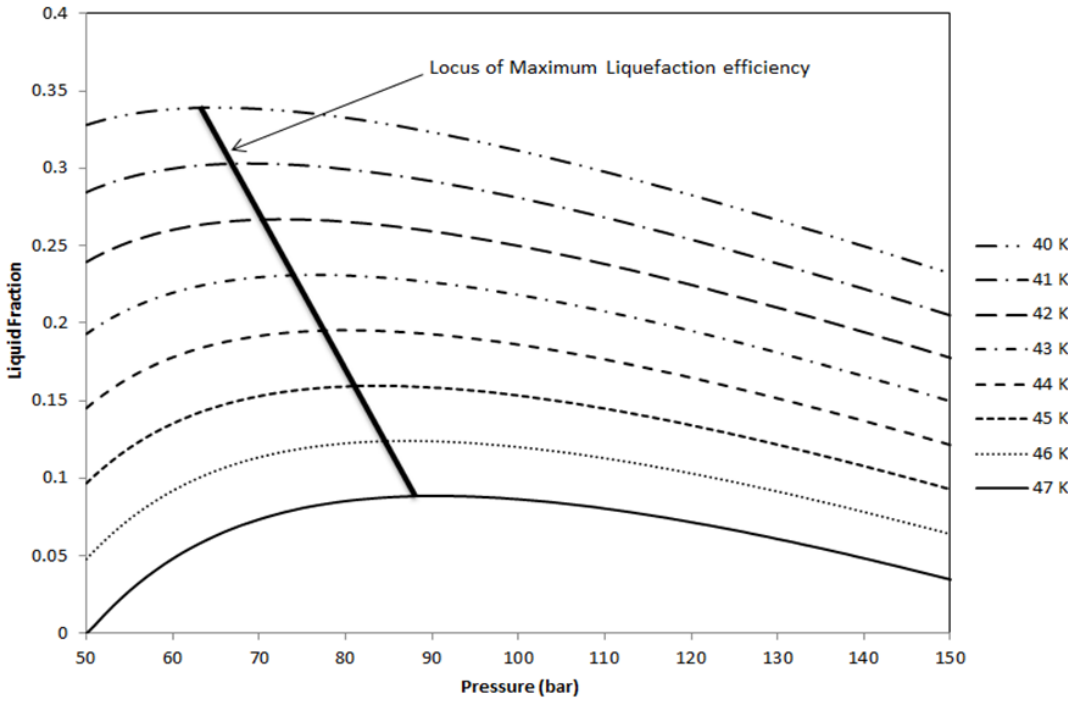

Fig. 8. The estimated hydrogen liquid fraction at the expansion valve outlet versus operational pressure at various input temperatures and output pressure of 1.2 bar.

flow entering the expansion valve are located on the locus of maximum hydrogen liquefaction.

In order to determine the temperature and pressure of streams joining the recuperative heat exchanger, two parameters of temperature approach and energy balance along with the Joule-Thomson effect upon the expansion valve must be considered. Temperature approach can be studied by simultaneously establishing the energy balance around the recuperative heat exchanger and considering Joule-Thomson effect. The calculations were done using equation (5). This equation correlates the above-mentioned parameters together. Temperature approach occurs at the warm end of the recuperative heat exchanger. Therefore, considering temperature approach equal to 3 K, the value of $T_{o\text{-}out}$ is equal to 66K. Actually, temperature approach as a key parameter determining the value of $T_{o\text{-}out}$ in equation (5). In other words, if we define a new variable as $\Delta h = (T_{i\text{-}in} - T_{o\text{-}out})$, then equation (5) can be changed to equation (7) as follows:

(7)

$$m_i C_i \left(T_{i-in} - T_{i-out}\right) = m_i (1 - x[T_{i-out}, P_{i-out}]) C_o \left(T_{i-in} - \Delta_h - T_{o-in}\right)$$

Where, Δ_h is the temperature approach in the recuperative heat exchanger. The temperature approaches for the recuperative heat exchanger at pressures between 50 to 150 bar versus the temperature of warm gas leaving the recuperative heat exchanger ($T_{I\text{-}OUT}$, the stream entering the expansion valve) were evaluated using MATLAB programming. The plots are presented in Figure 9. The plots can be used as an efficient tool to determine the optimum pressure and temperature of a stream entering the expansion. The first step of process design for a hydrogen liquefaction unit is the selection of appropriate pressure for the system. The pressure of the system should be selected based on the liquefaction methods (Linde-Hampson, Claude, etc.), volume of equipment, hardware facilities, safety system, etc. In the current study, pressure of 80 bar was selected because of the safety aspects and technical limitations of our small hydrogen liquefier. Considering heat exchanger effectiveness, a temperature approach of 3 K was selected. Considering a temperature approach of 3 K, operational pressure of 80 bar, and plots shown

in Fig. 9, the temperature of the stream entering the expansion valve was evaluated around 44.7 K. The temperature of 44.7 K (~45 K) and pressure of 80 bar demonstrate a point on the locus of maximum liquefaction in Fig. 8. This means that the temperature of 44.7 K is an appropriate temperature for a stream entering the expansion valve at the selected pressure. As can be seen in Fig. 10, one stream has an unknown value. The temperature of this stream can be simply evaluated by considering the temperature approach in the recuperative heat exchanger. Since the hydrogen heat capacity variation is not linear along the heat exchanger tube, the unknown temperature must be evaluated by considering the variable heat capacity. This parameter was considered in the calculations performed in the individual differential segments.

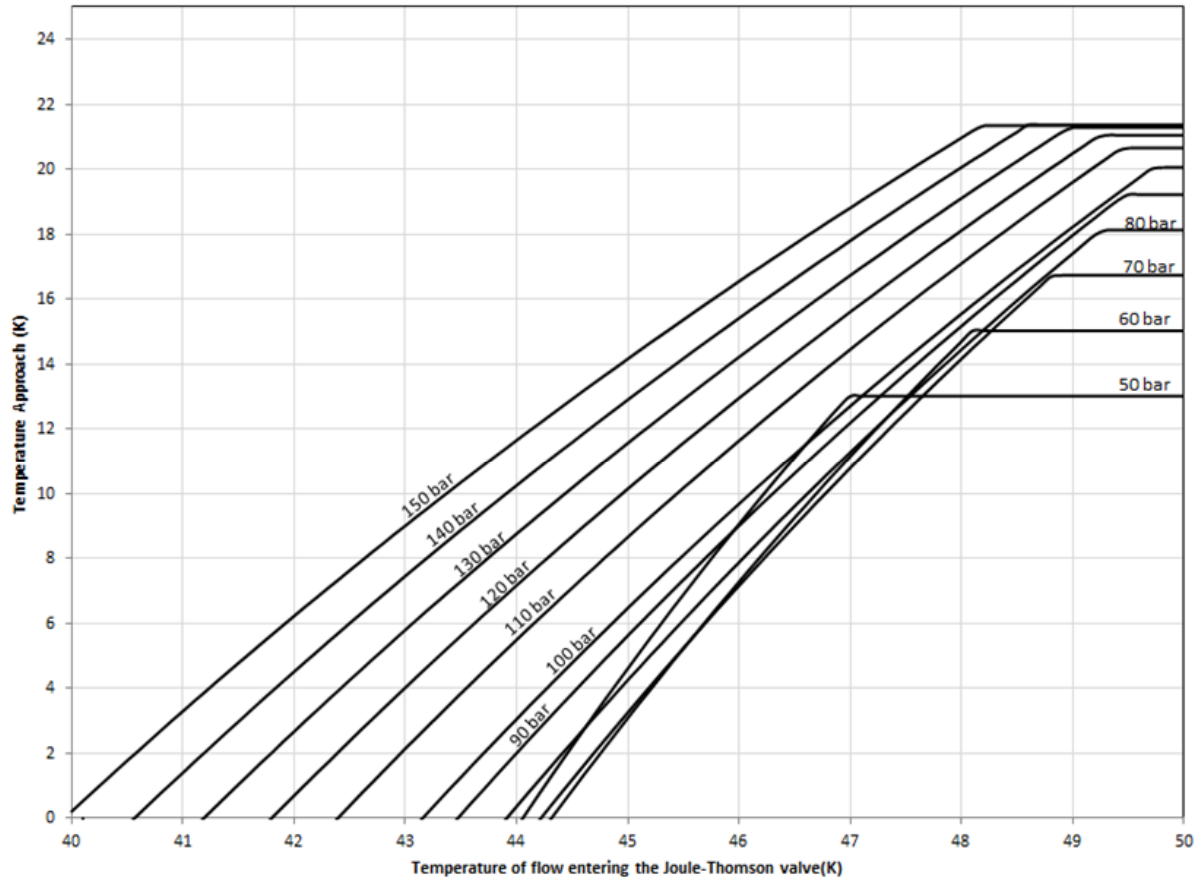

Fig. 9. The temperature approach of a recuperative heat exchanger versus the temperature of the high pressure stream leaving the heat exchanger (entering the Joule-Thomson valve) at various operational pressures (precooling temperature of 69 K).

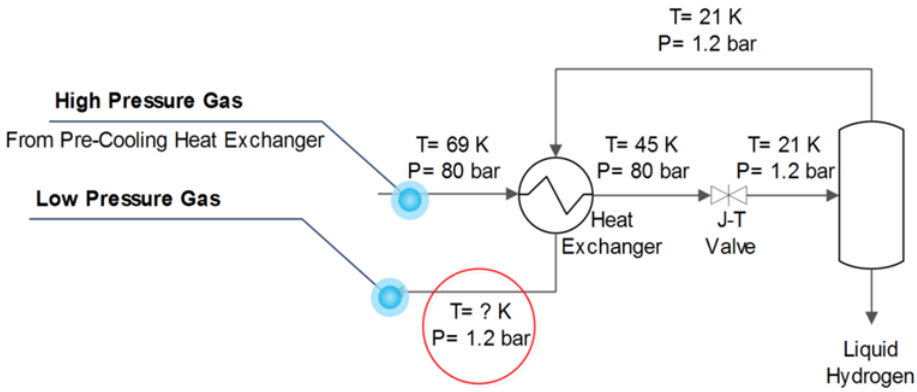

Fig. 10. The evaluated temperatures of various streams in the Joule-Thomson cooling system.

3.2. Configuration of Streams within the Heat Exchanger

The JTC systems operate at very low temperatures. Therefore, heat in-leak from surroundings generally takes place in the recuperative heat exchanger. Heat in-leak can prevent normal operating of a recuperative heat exchanger. In order to eliminate the negative effect of heat in-leak, the external surface area of a heat exchanger must be as small as possible. For this reason, the appropriate length of the heat exchanger must be determined accurately. The temperature profiles of high and low pressure streams obtained from mathematical simulation were shown in Fig.11. Fig. 11-A shows the temperature profiles of high and low pressure streams in which the high pressure hydrogen (warm gas) flows within the inner tube and the low pressure hydrogen (cold stream) flows within the annulus. Fig. 11-B shows the reversed configuration of streams shown in Fig. 11-A.

As can be seen, the heat exchanger length in Fig. 11-A are greater than that in Fig. 11-B. This means that the configuration of streams in which the high pressure gas flows within the annulus is favorable due to lower heat leakage from the surroundings. For a heat exchanger with different geometries and mass flow rates, the results can be quite different. Therefore, the configuration of streams must be performed before cryogenic heat exchanger design to reduce the heat exchanger length and heat leakage from the surroundings.

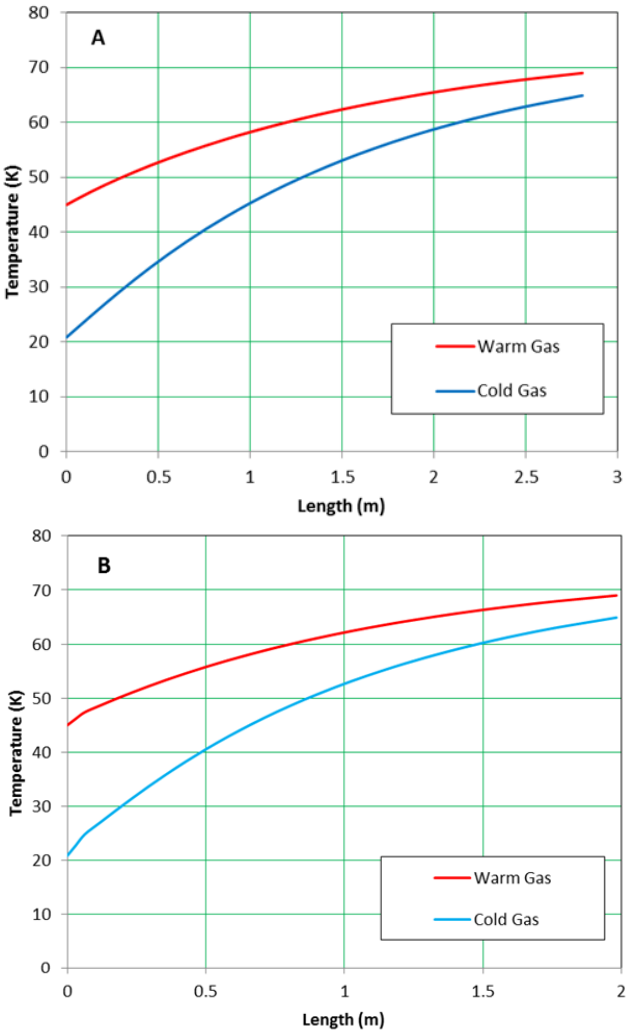

Fig. 11. The temperature profiles of a helically coiled tube in a tube recuperative heat exchanger. A) High pressure hydrogen flows within the inner tube. B) High pressure hydrogen flows within the annular.

3.3. Influence of Heat Exchanger Effectiveness on the Overall Efficiency of Unit

According to the literature, the minimum effectiveness of a recuperative heat exchanger operating in a hydrogen liquefier must be greater than 95%, otherwise the liquefaction of hydrogen does not take place. The liquid fraction of hydrogen at the expansion valve outlet was obtained using the equation of state and energy balance around the system at various pre-cooling temperatures and heat exchanger effectiveness. The results are shown in Fig. 12.

As can be seen, lower heat exchanger effectiveness

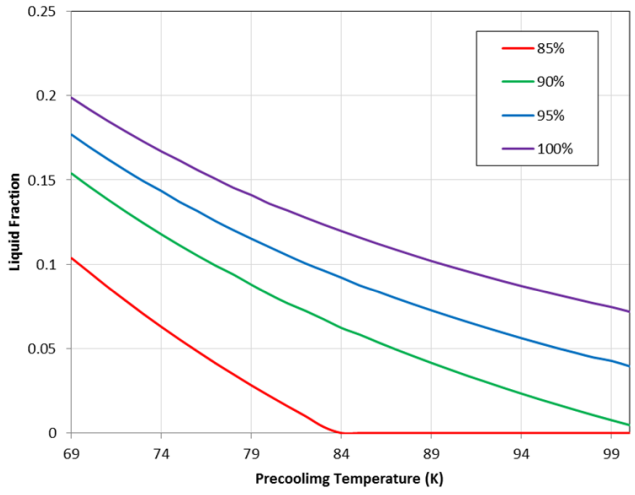

Fig. 12. The values of liquid fraction versus precooling temperature at different heat exchanger effectiveness.

leads to needing a lower pre-cooling temperature at the same liquid fraction value. For example, a recuperative heat exchanger with an effectiveness of 85% and a pre-cooling temperature of 84 K cannot be used in the hydrogen liquefier, because the liquid fraction at the expansion valve outlet will be zero, while a recuperative heat exchanger with an effectiveness of 95 % and the same pre-cooling temperature can liquefy 10% of the hydrogen. Two process parameters can be used to improve the efficiency of a hydrogen liquefier; decreasing the pre-cooling temperature and increasing the operational pressure of system. Decreasing the pre-cooling temperature is limited to the temperature of the LN_2 bath (in the case of our study). The triple point of LN_2 is around 65 K and further increasing the vacuum results in solid nitrogen formation. The formation of solid nitrogen is undesirable because of the inferior heat transfer conditions between tube wall and solid nitrogen compared with LN_2 bath . This means that solid nitrogen with a lower operational temperature, with respect to LN_2, cannot be used as an efficient pre-cooling refrigerant. Fig.13 shows the variation of liquid fraction versus precooling temperatureat different operational pressures. As can be seen, increasing the pressure improves the liquid fraction of hydrogen at the expansion valve outlet. The increased liquid fraction demonstrates that increasing the pressure can be used as an operational parameter to improve the hydrogen liquefier efficiency. Although, increasing the pressure improves the liquid fraction, the improvement is negligible at pressures higher than 100 bar. Considering the higher cost for obtaining higher pressures and safety aspects, increasing the operational pressure is not a desirable parameter to improve liquid fraction. Therefore, decreasing the pre-cooling temperature and increasing the operational pressure cannot be used to improve hydrogen liquefier efficiency. This means that the recuperative heat exchanger effectiveness is a very important parameter and should be considered in the manufacturing step.

4. Conclusions

The JTC system is the main part of the cryogenic liquefaction processes. Based on the discussion presented in this paper, determining the temperatures and pressures for various streams in JTC systems by simple energy balance around the recuperative heat exchanger is not possible, since several parameters

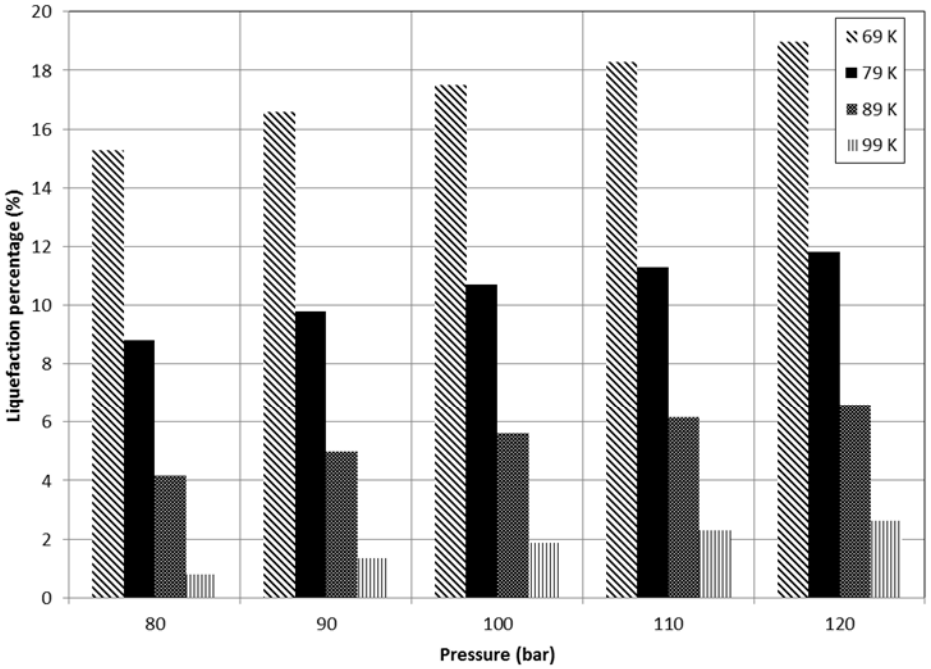

Fig. 13. The variation of liquid fraction versus precooling temperature at different pressures.

such as temperature approach, operational pressure, and inlet temperature of the Joule-Thomson valve must be considered simultaneously. These parameters were used to determine the temperature and pressure of various streams for a recuperative heat exchanger with a straightforward method and new approach. In accordance with mathematical modeling performed on the recuperative heat exchanger, it is better to flow low pressure hydrogen inside the inner tube and high pressure hydrogen within the annulus. This arrangement results in needing a shorter length for heat exchanger tubes compared with the reverse arrangement. The efficiency of a Joule-Thomson cooling system was studied, and two parameters of operational pressure and pre-cooling temperature were considered to improve the system. Finally, it was concluded that these process parameters cannot significantly improve the liquid fraction at the expansion valve outlet.

Nomenclature

P	Pressure, bar
T	Temperature, K
ρ	Density, $kg.m^{-3}$
R	Universal constant of gases, $kJ.kmol^{-1}.K^{-1}$
γ	Ratio of heat capacities, dimensionless
G	Correlation parameter of the MBWR equation of state
Cp_{HP}	Mass heat capacity of hydrogen at 80 bar, $kJ.kg^{-1}.K^{-1}$
Cp_{LP}	Mass heat capacity of hydrogen at 1.2 bar, $kJ.kg^{-1}.K^{-1}$
μ_{HP}	Viscosity of hydrogen at 80 bar, $Pa.s^{-1}$
μ_{LP}	Viscosity of hydrogen at 1.2 bar, $Pa.s^{-1}$
ρ_{HP}	Density of hydrogen at 80 bar, $kg.m^{-3}$
ρ_{LP}	Density of hydrogen at 1.2 bar, $kg.m^{-3}$
k_{HP}	Thermal conductivity of hydrogen at 80 bar, $kJ.m^{-1}.K^{-1}$
k_{LP}	Thermal conductivity of hydrogen at 1.2 bar, $kJ.m^{-1}.K^{-1}$
Nu_{ave}	Nusselt number, dimensionless
De	Dean number, dimensionless
Pr	Prandtl number, dimensionless
d	Diameter of tube, m
Re	Reynolds number, dimensionless
D_{coil}	Diameter of coil, m
m	Mass flow, $kg.s^{-1}$
x	Liquid fraction, dimensionless
μ_{J-T}	Joule-Thomson coefficient, $K.Pa^{-1}$
h_{HP}	Convective heat transfer coefficient the high pressure gas, $kJ.m^{-2}.K^{-1}$
h_{LP}	Convective heat transfer coefficient the low pressure gas, $kJ.m^{-2}.K^{-1}$
t	Diameter of tube wall, m

Subscript

HP	High Pressure
LP	Low Pressure
i	Inner
o	outer

5. References

[1] Zhu W., White M. J., Nellis G. F., Klein S. A., Gianchandani Y. B. "A Joule-Thomson cooling system with a Si/glass heat exchanger for 0.1–1 w heat loads. in Solid-State Sensors", Actuators and Microsystems Conference, TRANSDUCERS, International. IEEE, 2009, 2417.

[2] Maytal B. Z., Nellis G., Klein S.,Pfotenhauer J., "Elevated-pressure mixed-coolants Joule–Thomson cryocooling", Cryogenics, 2006, 46(1): 55.

[3] Croft A., "The new hydrogen liquefier at the Clarendon Laboratory", Cryogenics, 1964, 4(3): 143.

[4] Prina M., Borders J., Bhandari P., Morgante G., Pearson D., Paine C., "Low-heat input cryogenic temperature control with recuperative heat-exchanger in a Joule Thomson cryocooler", Cryogenics, 2004, 44(6):595.

[5] Barron R. F., Nellis G.,Pfotenhauer J. M., Cryogenic heat transfer. CRC Press, 1999.

[6] Stephens S., "Advanced design of Joule-Thomson coolers for infra-red detectors", Infrared Physics, 1968, 8(1): 25.

[7] Chien S., Chen L., Chou F., "A study on the transient characteristics of a self-regulating Joule-Thomson cryocooler", Cryogenics, 1996, 36(12): 979.

[8] Levenduski R.,Scarlotti R.D. "Development of a Joule-Thomson cryocooler for space applications", in SPIE's International Symposium on Optical Engineering and Photonics in Aerospace Sensing. International Society for Optics and Photonics, 1994, 109.

[9] Chua H. T., Wang X., Teo H. Y., "A numerical study of the Hampson-type miniature Joule–Thomson cryocooler", Int. J. Heat Mass Transfer, 2006, 49(3): 582.

[10] Damle R.,Atrey M., "Transient simulation of a miniature Joule-Thomson (JT) cryocooler with and without the distributed JT effect", Cryogenics, 2014, 65:49.

[11] Pacio J. C., Dorao C. A., "A review on heat exchanger thermal hydraulic models for cryogenic applications", Cryogenics, 2011, 51(7): 366.

[12] Aminuddin M.,Zubair S.M., "Characterization of various losses in a cryogenic counterflow heat exchanger", Cryogenics, 2014, 64: 6477.

[13] Krishna V., Spoorthi S., Hegde P. G.,Seetharamu K., "Effect of longitudinal wall conduction on the performance of a three-fluid cryogenic heat exchanger with three thermal communications", Int. J. Heat Mass Transfer, 2013, 62: 567.

[14] Gupta P. K., Kush P.,Tiwari A., "Second law analysis of counter flow cryogenic heat exchangers in presence of ambient heat-in-leak and longitudinal conduction through wall", Int. J. Heat Mass Transfer, 2007, 50(23): 4754.

[15] Nellis G., "A heat exchanger model that includes axial conduction, parasitic heat loads, and property variations", Cryogenics, 2003, 43(9): 523.

[16] Narayanan S. P.,Venkatarathnam G., "Performance of a counterflow heat exchanger with heat loss through the wall at the cold end", Cryogenics, 1999, 39(1): 43.

[17] Ranganayakulu C., Seetharamu K.,Sreevatsan K., "The effects of longitudinal heat conduction in compact plate-fin and tube-fin heat exchangers using a finite element method", Int. J. Heat Mass Transfer, 1997, 40(6):1261.

[18] Damle R., Atrey M., "The cool-down behaviour of a miniature Joule–Thomson (J–T) cryocooler with distributed J–T effect and finite reservoir capacity", Cryogenics, 2015, 71: 47.

[19] Chou F. C., Pai C. F., Chien S.,Chen J., "Preliminary experimental and numerical study of transient characteristics for a Joule-Thomson cryocooler", Cryogenics, 1995, 35(5): 311.

[20] Tzabar N.,Kaplansky A., "A numerical cool-down analysis for Dewar-detector assemblies cooled with Joule–Thomson cryocoolers", Int. J. Ref., 2014, 44: 56.

[21] Hong Y. J., Park S. J., Kim H.-B.,Choi Y.-D., "The cool-down characteristics of a miniature Joule–Thomson refrigerator", Cryogenics, 2006, 46(5): 391.

[22] Valenti G., Macchi E.,Brioschi S., "The influence of the thermodynamic model of equilibriumhydrogen on the simulation of its liquefaction", Int. J. Hydrogen Energy, 2012, 37: 10779.

[23] Younglove B. A., "Thermophysical properties of fluids. I. Argon, ethylene, parahydrogen, nitrogen, nitrogen trifluoride, and oxygen". 1982,

[24] McCarty R. D., Hord J., Roder H., Selected properties of hydrogen (engineering design data). National Engineering Lab.(NBS), Boulder, CO (USA), 1981,

[25] Xin R.,Ebadian M., "The effects of Prandtl numbers on local and average convective heat transfer characteristics in helical pipes", J. Heat Transfer, 1997, 119(3): 467.